The Plant Cell, Vol. 30: 871–888, April 2018, www.plantcell.org © 2018 ASPB.

GRAIN SIZE AND NUMBER1 Negatively Regulates the OsMKKK10-OsMKK4-OsMPK6 Cascade to Coordinate the Trade-off between Grain Number per Panicle and Grain Size in Rice

Tao Guo,[a,b] Ke Chen,[a,b] Nai-Qian Dong,[a,b] Chuan-Lin Shi,[a,b] Wang-Wei Ye,[a] Ji-Ping Gao,[a] Jun-Xiang Shan,[a,1] and Hong-Xuan Lin[a,b,c,1]

[a] National Key Laboratory of Plant Molecular Genetics, CAS Centre for Excellence in Molecular Plant Sciences and Collaborative Innovation Center of Genetics and Development, Shanghai Institute of Plant Physiology and Ecology, Shanghai Institute for Biological Sciences, Chinese Academic of Sciences, Shanghai 200032, China
[b] University of the Chinese Academy of Sciences, Beijing 100049, China
[c] School of Life Science and Technology, ShanghaiTech University, Shanghai 201210, China

ORCID IDs: 0000-0003-2538-7793 (K.C.); 0000-0002-8968-4423 (J.-P.G.); 0000-0002-7235-4225 (J.-X.S.); 0000-0002-2818-023X (H.-X.L.)

Grain number and size are interactive agronomic traits that determine grain yield. However, the molecular mechanisms responsible for coordinating the trade-off between these traits remain elusive. Here, we characterized the rice (*Oryza sativa*) *grain size and number1* (*gsn1*) mutant, which has larger grains but sparser panicles than the wild type due to disordered localized cell differentiation and proliferation. *GSN1* encodes the mitogen-activated protein kinase phosphatase OsMKP1, a dual-specificity phosphatase of unknown function. Reduced expression of *GSN1* resulted in larger and fewer grains, whereas increased expression resulted in more grains but reduced grain size. GSN1 directly interacts with and inactivates the mitogen-activated protein kinase OsMPK6 via dephosphorylation. Consistent with this finding, the suppression of mitogen-activated protein kinase genes *OsMPK6*, *OsMKK4*, and *OsMKKK10* separately resulted in denser panicles and smaller grains, which rescued the mutant *gsn1* phenotypes. Therefore, OsMKKK10-OsMKK4-OsMPK6 participates in panicle morphogenesis and acts on a common pathway in rice. We confirmed that GSN1 is a negative regulator of the OsMKKK10-OsMKK4-OsMPK6 cascade that determines panicle architecture. The GSN1-MAPK module coordinates the trade-off between grain number and grain size by integrating localized cell differentiation and proliferation. These findings provide important insights into the developmental plasticity of the panicle and a potential means to improve crop yields.

INTRODUCTION

Rice (*Oryza sativa*), the number one staple cereal crop worldwide, feeds more than half of the global population every day. Yield in rice depends on tiller number, grain weight, and the number of grains per panicle. Grain number per panicle is determined by the number of primary and secondary branches, and grain weight is determined by grain size and the degree of filling (Xing and Zhang, 2010). The genetic and molecular bases of these agronomic traits have been extensively studied via mapping of quantitative trait loci combined with mutant identification using multiple genetic resources. Considerable progress has been made in understanding the molecular mechanisms of rice panicle morphogenesis and reproductive organ development, which are controlled by diverse proteins and unknown signaling pathways (Zhang and Yuan, 2014; Zuo and Li, 2014). In particular, several genes associated with grain number (Ashikari et al., 2005; Kurakawa et al., 2007; Huang et al., 2009; Oikawa and Kyozuka, 2009; Wu et al., 2016; Huo et al., 2017) and grain size (Song et al., 2007; Mao et al., 2010; Li et al., 2011; Qi et al., 2012; Hu et al., 2015; Si et al., 2016) have been identified and characterized in rice; these genes strongly influence cell differentiation and either cell proliferation or cell expansion, depending on phytohormones or other unidentified signaling molecules. Rice has a determinate inflorescence, in which the meristems differentiate into primary branch meristems attached to the central rachis, which then form several secondary branch meristems (Zhang and Yuan, 2014). The spikelet meristems form directly on primary and secondary branches, which determines the final number of grains per panicle. The differentiated spikelets develop and produce terminal floral organs with palea and lemma, which determine grain size. These spatiotemporal programmed cellular processes contribute interactively to rice panicle architecture. In many plant species, there is a negative evolutionary correlation between seed number and seed size (Sadras, 2007). Nevertheless, the explicit molecular mechanisms coordinating the trade-off between grain number per panicle and grain size in rice remain largely unknown.

[1] Address correspondence to hxlin@sibs.ac.cn or jxshan@sibs.ac.cn.
The authors responsible for distribution of materials integral to the findings presented in this article in accordance with the policy described in the Instructions for Authors (www.plantcell.org) are: Hong-Xuan Lin (hxlin@sibs.ac.cn) and Jun-Xiang Shan (jxshan@sibs.ac.cn).
www.plantcell.org/cgi/doi/10.1105/tpc.17.00959

IN A NUTSHELL

Background: Rice is one of the main staple cereal crops worldwide that feeds more than half of the global population every day. Its yield depends on tiller number, grain (seed) weight, and the number of grains per panicle. Grain number per panicle is determined by the number of primary and secondary branches, and grain weight is determined by grain size and the degree of filling. Rice is also a good model plant. It is well known that there is a negative correlation between seed number and seed size in many plants, and this has a central evolutionary role. However, we don't know the intrinsic mechanisms by which rice can determine the optimal grain number per panicle and grain size and maintain equilibrium of reproductive organ development.

Question: We wanted to know the intrinsic mechanisms that coordinate the trade-off between grain number per panicle and grain size in rice. Which biological molecules confer the grain number and grain size of rice plant exactly almost at the same time?

Findings: We found that the *GSN1* gene of rice acts like a "molecular brake" that determines the grain number per panicle and grain size exactly, and the alteration of this gene directly influenced panicle patterning and grain shape. We discovered that the rice *grain size and number1* (*gsn1*) mutant has larger but fewer grains due to inactivation and weakened function of the *GSN1* gene. Surprisingly, when we enhanced the function of *GSN1* or elevated its endogenous level in rice, these plants had smaller but more grains per panicle.

Next steps: Scientists aim to improve crop yields to produce new crops with increased number and size of grains. However, the negative correlation between grain number and size restricts panicle patterning. Our work demonstrates a key element in this developmental process, *GSN1*, which could help crop scientists to cultivate high-yielding varieties using gene-editing technology.

Mitogen-activated protein kinase (MAPK) cascades are highly conserved, ubiquitous signaling pathways in eukaryotes (Widmann et al., 1999) that relay and amplify signals via a set of three types of activated protein kinases: MAPK kinase kinase (MKKK, or MEKK), MAPK kinase (MKK, or MEK), and MAPK (Rodriguez et al., 2010). MKKK receives signals from the topmost receptor or sensor to activate MKK, and the activated MKK then activates MAPK. This cascade depends on sequential phosphorylation and leads to the altered activities of substrates through phosphorylation, which regulates cell proliferation and differentiation and the coordination of responses to environmental inputs (Xu and Zhang, 2015). Plant MAPK signaling modules play essential roles in multiple processes, including immunity, stress responses, and developmental programs (Wang et al., 2007, 2017; Lampard et al., 2008; Kong et al., 2012; Meng et al., 2012; Meng and Zhang, 2013; Xu and Zhang, 2015). Components of the rice MAPK cascades, OsMKK4 and OsMAPK6, have recently been characterized, both of which influence grain size, depending on cell proliferation (Duan et al., 2014; Liu et al., 2015). However, the negative regulators of MAPK cascades in crops have not yet been identified.

To investigate the genetic and molecular mechanisms underlying the trade-off between grain number per panicle and grain size in rice, we screened an ethyl methanesulfonate (EMS) mutant library for presumed panicle phenotypes. Here, we report the isolation and characterization of a rice mutant, *grain size and number1* (*gsn1*), that displays increased grain size and reduced grain number per panicle compared with the wild type. We demonstrate that GSN1 acts as a negative regulator of the OsMKKK10-OsMKK4-OsMPK6 cascade by inducing specific dephosphorylation of OsMPK6 to coordinate the trade-off between grain number per panicle and grain size. Thus, our findings establish a molecular understanding of trade-offs in rice panicle development and provide a potential opportunity to improve crop yields.

RESULTS

gsn1 Has Larger Grain Size and Reduced Grain Number

To investigate the genetic association between grain size and grain number, we treated the mutagenic elite *indica* rice variety Fengaizhan-1 (FAZ1) with EMS and isolated the *gsn1* mutant, which displays distinctly larger grain size but reduced grain number per panicle and larger floral organs than the wild type without additional phenotypes (Figures 1A to 1H). The average grain length, width, and 1000-grain weight in the *gsn1* mutant were markedly increased, but grain number per panicle and setting percentage were dramatically reduced compared with wild-type FAZ1 (Figures 1I to 1M; Supplemental Figures 1A, 1B, and 1E), which resulted in reduced grain yield per plant (Figure 1N). The reduced numbers of both primary and secondary branches, rather than panicle size, directly determined the total spikelet number in the *gsn1* mutant (Figures 1O to 1Q). Taken together, these results imply that *GSN1* specifically influences panicle and spikelet development in rice.

Map-Based Cloning of *GSN1*

We isolated the *GSN1* gene via map-based cloning using an F2 population derived from a cross between the *gsn1* mutant line and the *japonica* rice variety, Zhonghua-11 (ZH11). The *GSN1* locus was initially mapped to the short arm of chromosome 5 between the marker loci G05220 and G05591 using 682 homozygous F2 plants and was then fine-mapped to a 17.5-kb region between marker loci G05333 and G05340 that contains two open reading frames (ORFs), LOC_Os05g02490 and LOC_Os05g02500 (Figure 2A). Comparison of the genomic DNA sequences of the FAZ1 and *gsn1* alleles revealed that the allele from *gsn1* has a single C-to-T

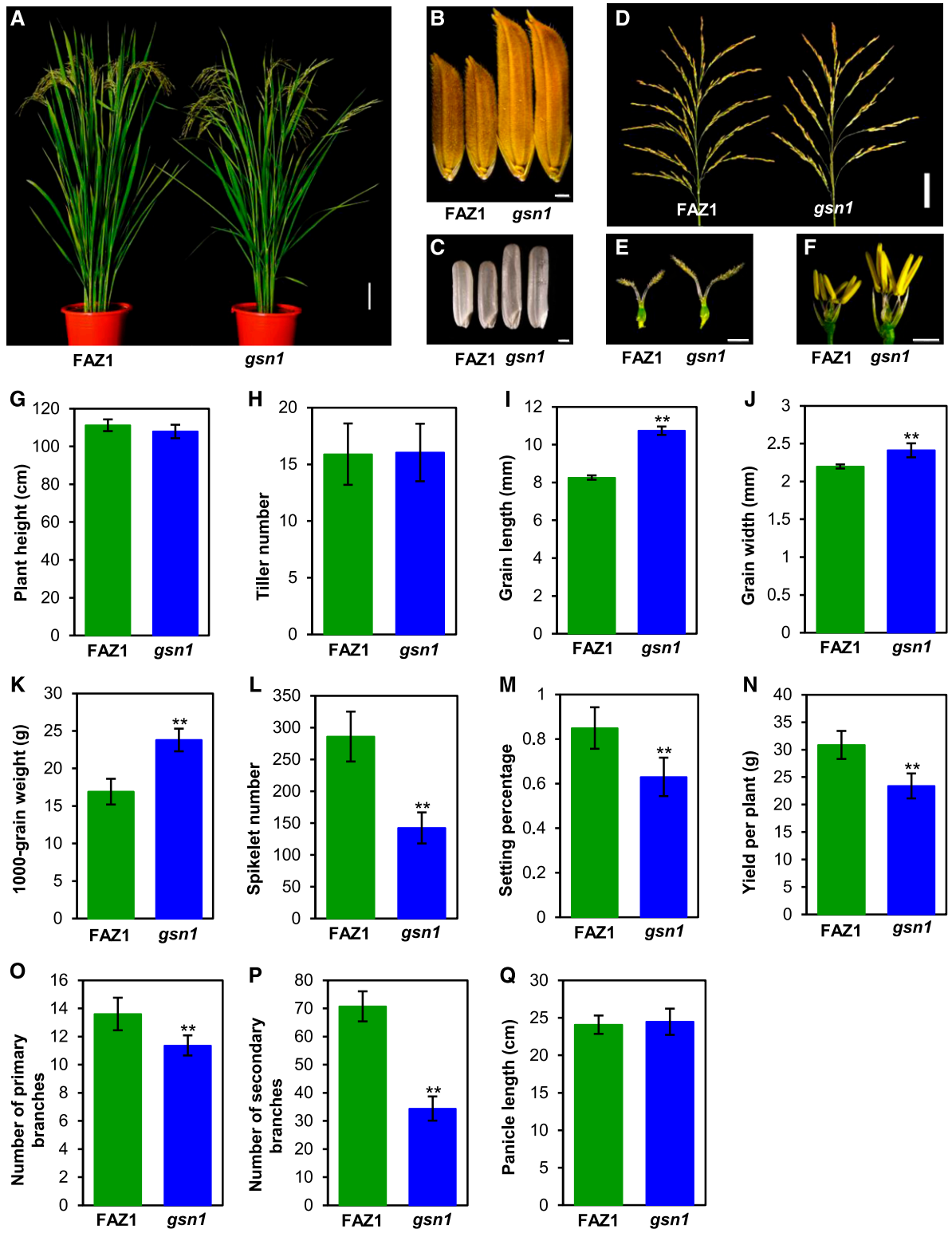

Figure 1. Characterization of the *gsn1* Mutant, Which Exhibits Increased Grain Size and Reduced Grain Number per Panicle.

(A) Plant architecture of wild-type FAZ1 and mutant *gsn1* plants at the reproductive stage. Bar = 10 cm.
(B) Mature paddy rice grains from FAZ1 and *gsn1*. Bar = 1 mm.
(C) Brown rice grains from FAZ1 and *gsn1*. Bar = 1 mm.

nucleotide mutation at position 437 in the candidate gene LOC_Os05g02500, which is predicted to encode a MAPK phosphatase OsMKP1, the dual-specificity phosphatase with a PTPc/DSPc (Protein Tyrosine Phosphatase catalytic/Dual Specific Phosphatase catalytic) domain and a GEL (Gelsolin) domain (Figure 2A). Protein sequence alignment showed that this mutation directly leads to a serine-to-phenylalanine change at amino acid S146, which is a conserved residue, and that GSN1 shares high amino acid sequence identity with its homologs in monocots and dicots (Figure 2B). These results indicate that LOC_Os05g02500 (OsMKP1) represents the only candidate gene for *GSN1*.

To further confirm the identity of the candidate gene, we performed a genetic complementation test in which a DNA fragment from the wild-type FAZ1 containing the putative promoter region, the entire ORF, and the 3′ untranslated region of *GSN1* was introduced into the *gsn1* mutant via *Agrobacterium tumefaciens*-mediated transformation. All positive transgenic lines harboring the full-length *GSN1* transgene showed completely wild-type phenotypes with respect to grain number per panicle and grain size (Figures 2C and 2D; Supplemental Figures 2A and 2D to 2F). Knockdown of *GSN1* using an artificial microRNA in FAZ1, which reduced the levels of endogenous gene expression, produced plants with phenotypes similar to those of the *gsn1* mutant (Figures 2E to 2J; Supplemental Figures 2B, 2G, and 2J), but this is in contrast to the phenotypes of *GSN1* overexpression lines in FAZ1, which have reduced grain size and increased grain number per panicle (Figures 2G, 2H, 2K, and 2L; Supplemental Figures 2C, 2H, and 2K). In addition, we developed a nearly isogenic line, NIL (*gsn1*), with a very small chromosomal region carrying the *gsn1* allele in the *japonica* variety 95-22 genetic background from the BC_6F_2 generation, which displayed larger grain size and reduced grain number per panicle like the *gsn1* mutant (Supplemental Figure 3). These results demonstrate that *GSN1* is responsible for the alterations in grain size and grain number per panicle found in the *gsn1* mutant.

GSN1 Is a Negative Regulator of Grain Size but a Positive Regulator of Grain Number

To further confirm and estimate the genetic effect of *GSN1*, we performed a wide array of transgenic experiments using the *japonica* variety ZH11. The knockdown of *GSN1* using an artificial microRNA in ZH11 resulted in significantly increased grain size and reduced grain number per panicle (Supplemental Figures 4A and 4C to 4F), which is consistent with the phenotypes of transgenic lines produced by CRISPR/Cas9 genome editing, with distinct grain size and grain number per panicle, as well as very low fertility (Supplemental Figures 1C, 1D, 1F, 4B, and 4G to 4J). However, overexpression lines produced using the *GSN1* alleles from FAZ1 and ZH11 exhibited increased grain number per panicle and reduced grain size, which are completely the opposite panicle phenotypes compared with the *gsn1* allele $GSN1^{S146F}$ that resembles the $GSN1^{RNAi}$ lines expressing an artificial microRNA (Supplemental Figures 5A to 5J and 6A to 6J). Thus, we hypothesize that *GSN1* is both a negative regulator of grain size and a positive regulator of grain number per panicle and that the larger grains with high levels of exogenous *gsn1* allele expression resulted from dominant negative effects. Interestingly, only the repression of *GSN1* led to greatly reduced setting percentage similar to that of the *gsn1* mutant compared with the wild type, which implies that *GSN1* is required for both fertility and final grain number in rice (Supplemental Figures 1G to 1L). These results suggest that *GSN1* plays an interactive role in the trade-off between grain number per panicle and grain size.

GSN1 Influences Cell Proliferation instead of Cell Elongation to Control Organ Size

Given that the *gsn1* mutant has dramatically enlarged grains and floral organs, we examined the cell number and cell size of this line. We compared cross sections of the central parts of the spikelet hulls in FAZ1 and *gsn1* before heading to investigate the cellular basis of the increased organ size (Figures 3A to 3D). Our observations revealed that the outer parenchyma cells in *gsn1* significantly increased in number compared with the wild type, but the average cell length in *gsn1* was comparable to that in the wild type (Figure 3E). Since the mutant has large floral organs, we also examined the areas and cell numbers of the vascular bundles of the anther connectivum (which connects four different pollen sacs in FAZ1 and *gsn1*), finding that there were distinguishable differences between lines (Figure 3F). Furthermore, we examined the epidermal cells of mature grains and found that the average lengths of the outer epidermal cells of the spikelet hulls were not significantly different between *gsn1* and FAZ1 (Figures 3G and 3I). Similarly, the average length of the inner epidermal cells of *gsn1* spikelet hulls was comparable to that in FAZ1 (Figures 3H and 3J). Together, these results indicate that increased cell number, rather than cell size, contributes to the enlarged organs in the *gsn1* mutant.

Because of the similar life cycles and heading days of FAZ1 and *gsn1*, we hypothesized that an increased rate of cell division was responsible for the larger spikelet hulls of the mutant. Therefore, we analyzed the cell division rate in the spikelets of younger panicles by flow cytometry, finding that the percentage of G2/M

Figure 1. (continued).

(D) Mature panicles from FAZ1 and *gsn1* rice plants. Bar = 5 cm.
(E) Pistils of FAZ1 and *gsn1* flowers. Bar = 1 mm.
(F) Stamens of FAZ1 and *gsn1* flowers. Bar = 2 mm.
(G) to **(Q)** Comparisons between FAZ1 and *gsn1* for average plant height ($n = 20$ plants) **(G)**, average tiller number ($n = 20$ plants) **(H)**, average grain length ($n = 20$ plants) **(I)**, average grain width ($n = 20$ plants) **(J)**, 1000-grain weight ($n = 30$ plants) **(K)**, average spikelet number per panicle ($n = 20$ plants) **(L)**, setting percentage ($n = 20$ plants) **(M)**, average yield per plant ($n = 20$ plants) **(N)**, average number of primary branches ($n = 20$ plants) **(O)**, average number of secondary branches ($n = 20$ plants) **(P)**, and average panicle length ($n = 20$ plants) **(Q)**. Values are given as the mean ± SD. **$P < 0.01$ compared with the wild type using Student's *t* test.

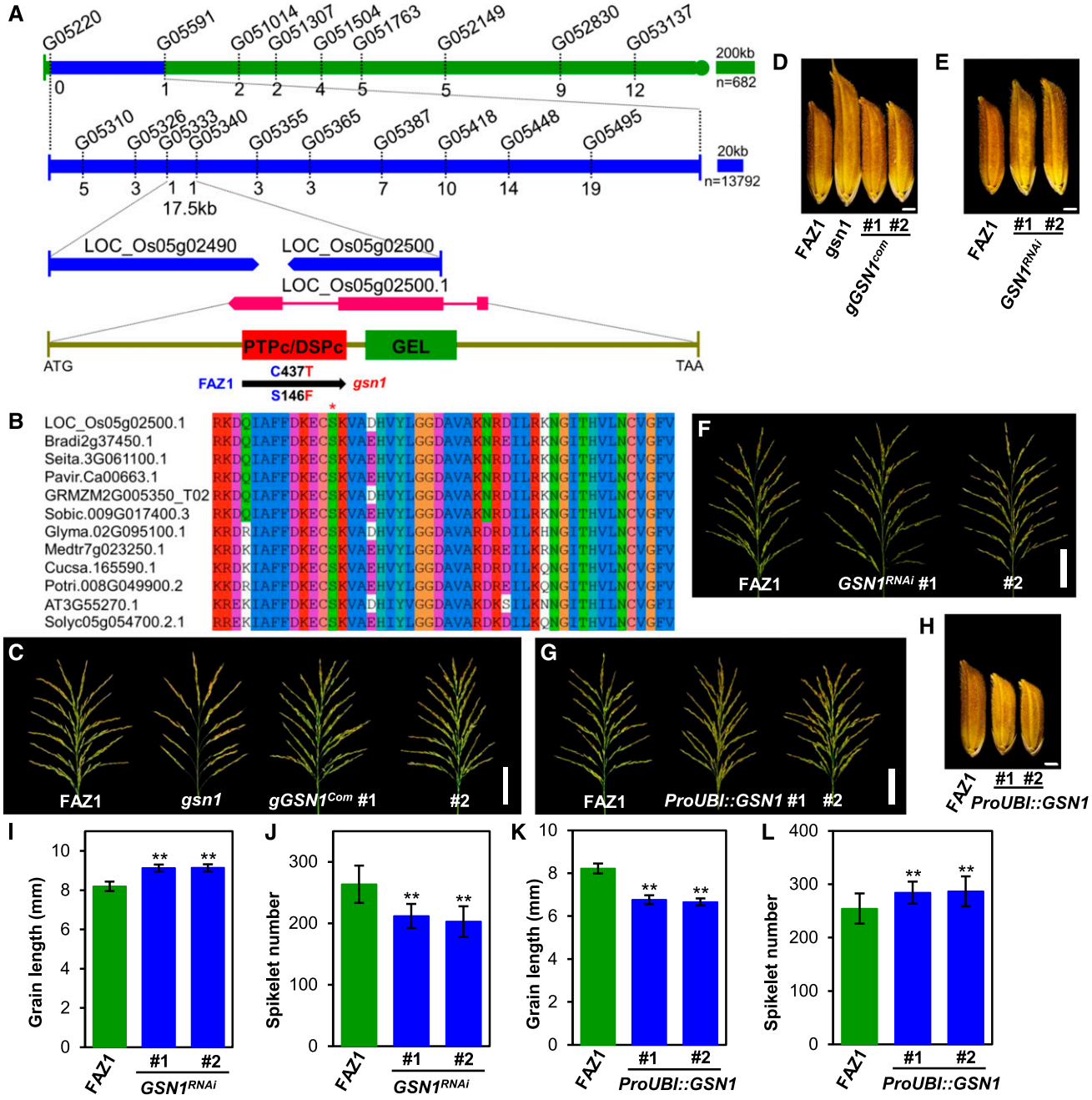

Figure 2. Map-Based Cloning of *GSN1* and Genetic Complementation.

(A) The *GSN1* locus was initially mapped to the short arm of chromosome 5 between the loci defined by markers G05220 and G05591 and then delimited to a 17.5-kb region between marker loci G05333 and G05340 that contained two ORFs. The numbers beneath the marker positions indicate the number of recombinants. Predicted protein structure of the first *GSN1* transcript; the red box indicates the PTPc/DSPc domain and the green box indicates the GEL domain. The start codon (ATG) and the stop codon (TGA) are also indicated. A single nucleotide mutation from C to T in *GSN1* results in a serine-to-phenylalanine change at S146 in the predicted PTPc/DSPc domain.

(B) Amino acid sequence alignment of the partially conserved PTPc/DSPc domain in six monocot and six dicot species. Identical and similar residues are shown in colored boxes. The asterisk indicates the site of the S146F mutation in the PTPc/DSPc domain at the highly conserved serine residue at position 146 in *gsn1*.

(C) Comparison of panicles between FAZ1, *gsn1*, and the T2 complementation transgenic lines *gGSN1*^{Com} #1 and *gGSN1*^{Com} #2 harboring the full-length *GSN1* gene in the mutant *gsn1* background. Bar = 5 cm.

(D) Mature grains of FAZ1, *gsn1*, *gGSN1*^{Com} #1, and *gGSN1*^{Com} #2. Bar = 1 mm.

phase cells with higher 4c DNA content was distinctly elevated in *gsn1* but that the percentage of G1 phase cells with 2c DNA content decreased after new cell cycles were initiated (Figures 3K and 3L). Hence, we conclude that cell division is more rapid in *gsn1* during spikelet development compared with the wild type. Consistent with the role of *GSN1* in the regulation of cell division, the expression levels of cell cycle-related genes and genes encoding several grain size regulators that influence cell proliferation were significantly upregulated in the spikelets of *gsn1* compared with FAZ1 (Supplemental Figure 7). Furthermore, the epidermal cell length of the spikelet hulls in different transgenic lines, including lines with repression or overexpression of *GSN1*, showed no obvious differences, but the cell number at the longitudinal axis increased dramatically in the repression lines and decreased in the overexpression lines (Supplemental Figures 8 and 9). In summary, these data show that *GSN1* influences cell proliferation instead of cell elongation to control floral organs size.

GSN1 Encodes a Dual-Specificity Phosphatase That Is Localized to the Cytoplasm

According to the Rice Genome Annotation Project and Phytozome databases, the *GSN1* gene (LOC_Os05g02500) is predicted to encode a dual-specificity phosphatase that contains PTPc/DSPc and GEL domains. Phosphatases are pivotal negative regulators of MAPK cascades, and studies in many model organisms have revealed that the dephosphorylation of MAPKs can be implemented via PTPs (protein tyrosine phosphatases), PSTPs (protein serine-threonine phosphatases) and DSPs (dual-specificity phosphatases) in vivo (Bartels et al., 2010). The MAPK phosphatases belong to a subgroup of the DSP family whose members specifically dephosphorylate both phosphotyrosine and phosphoserine/threonine residues within the activation motif of MAPKs (Luan, 2003). To determine whether the mutation of *GSN1* in *gsn1* abolishes its phosphatase activity, we expressed recombinant MBP-GSN1 and the mutated version MBP-GSN1^{S146F} in *Escherichia coli* and purified the fusion proteins for in vitro assays. Initially, the PNPP (*p*-nitrophenyl phosphate) was used as an artificial substrate to assay the phosphatase activity, but there was no significant activity in the recombinant GSN1 proteins, as determined based on absorbance at 405 nm (Figure 4A). Previous studies have indicated that DSPs usually prefer bulky polycyclic aryl phosphates and display weak enzyme activity toward simple aryl phosphates, such as PNPP, which likely contain shallower active site pockets (Yoo et al., 2004; Lee et al., 2008). Therefore, we used the bulky polycyclic aryl phosphate OMFP (3-*o*-methylfluorescein phosphate) as the substrate to assay the phosphatase activity of GSN1. We calculated the amount of 3-*o*-methylfluorescein (OMF) released by dephosphorylation based on the absorbance at 477 nm, which was used to characterize the enzymatic properties of GSN1 and to determine its kinetic parameters (Figures 4B and 4C). The phosphatase activities of both wild-type GSN1 and the mutated version GSN1^{S146F} determined using OMFP were markedly different, in that the mutated GSN1^{S146F} version is inactive in dephosphorylating OMFP (Figure 4B). These results imply that the conserved serine at position 146 is vital for the phosphatase activity of GSN1.

We also investigated the subcellular localization of GSN1 in *Nicotiana benthamiana* leaf cells and rice protoplasts. Fluorescence from GSN1-GFP fusion protein was observed at the cell periphery and in the cytoplasm of *N. benthamiana* leaf epidermal cells compared with the ubiquitous distribution of signals in the GFP positive control (Figure 4D). In agreement with this finding, fluorescence from GSN1-YFP fusion protein was mainly localized to the cytoplasm in rice protoplasts (Figure 4E). We also examined the expression pattern of *GSN1* using qRT-PCR and in transgenic plants expressing GUS fusion protein driven by the *GSN1* promoter. We found that *GSN1* was widely expressed in various vegetative and reproductive phase organs at a relatively high level in young panicles and spikelet hulls, which demonstrates that *GSN1* plays a role in panicle and spikelet development (Figures 4F and 4G; Supplemental Figures 10A to 10H).

GSN1 Interacts with and Inactivates OsMPK6 via Specific Dephosphorylation

Using a yeast two-hybrid assay, we found that GSN1 interacts strongly with OsMPK6 (LOC_Os06g06090), as does OsMPK1 (Reyna and Yang, 2006) (Figure 5A). To investigate the direct physical interaction between GSN1 and OsMPK6 in planta, we performed a biomolecular fluorescence complementation (BiFC) assay to stabilize the protein-protein interaction after recognition of the N-terminal and C-terminal parts of a split YFP. We produced DNA constructs in which GSN1 and OsMPK6 were fused separately to both the N-terminal (nYFP) and C-terminal fragments of YFP (cYFP). The nYFP-GSN1 fusion protein interacted with cYFP-OsMPK6, and cYFP-GSN1 interacted with nYFP-OsMPK6, as expected, but no interaction was detected between nYFP-GSN1 and the negative control, cYFP-OsHAL3 (Su et al., 2016) (Figure 5B), suggesting that GSN1 associates with OsMPK6 in vivo.

We further confirmed the interaction between GSN1 and OsMPK6 using coimmunoprecipitation assays in which GSN1-Flag and OsMPK6-Myc fusion protein constructs driven by the 35S promoter were coexpressed in *N. benthamiana* leaves. The proteins were immunoprecipitated with Flag beads and detected by immunoblot analysis using anti-Flag and anti-Myc antibodies.

Figure 2. (continued).

(E) Mature grains of FAZ1 and the two *GSN1^{RNAi}* transgenic lines. Bar = 1 mm.
(F) Panicles of FAZ1 and the RNAi transgenic lines *GSN1^{RNAi}* #1 and *GSN1^{RNAi}* #2 in FAZ1. Bar = 5 cm.
(G) Panicles of FAZ1 and the overexpression lines *ProUBI:GSN1* #1 and *ProUBI:GSN1* #2 in FAZ1. Bar = 5 cm.
(H) Mature grains of FAZ1 and the T2 overexpression transgenic lines *ProUBI:GSN1* #1 and *ProUBI:GSN1* #2 in FAZ1. Bar = 1 mm.
(I) and **(J)** Comparisons of average grain length **(I)** and spikelet number per panicle **(J)** between FAZ1 and the *GSN1^{RNAi}* lines (n = 10 plants).
(K) and **(L)** Comparisons of average grain length **(K)** and spikelet number per panicle **(L)** between FAZ1 and the *ProUBI:GSN1* lines (n = 15 plants).
Values in **(I)** to **(L)** are given as the mean ± SD. **$P < 0.01$ compared with the wild type using Student's t test.

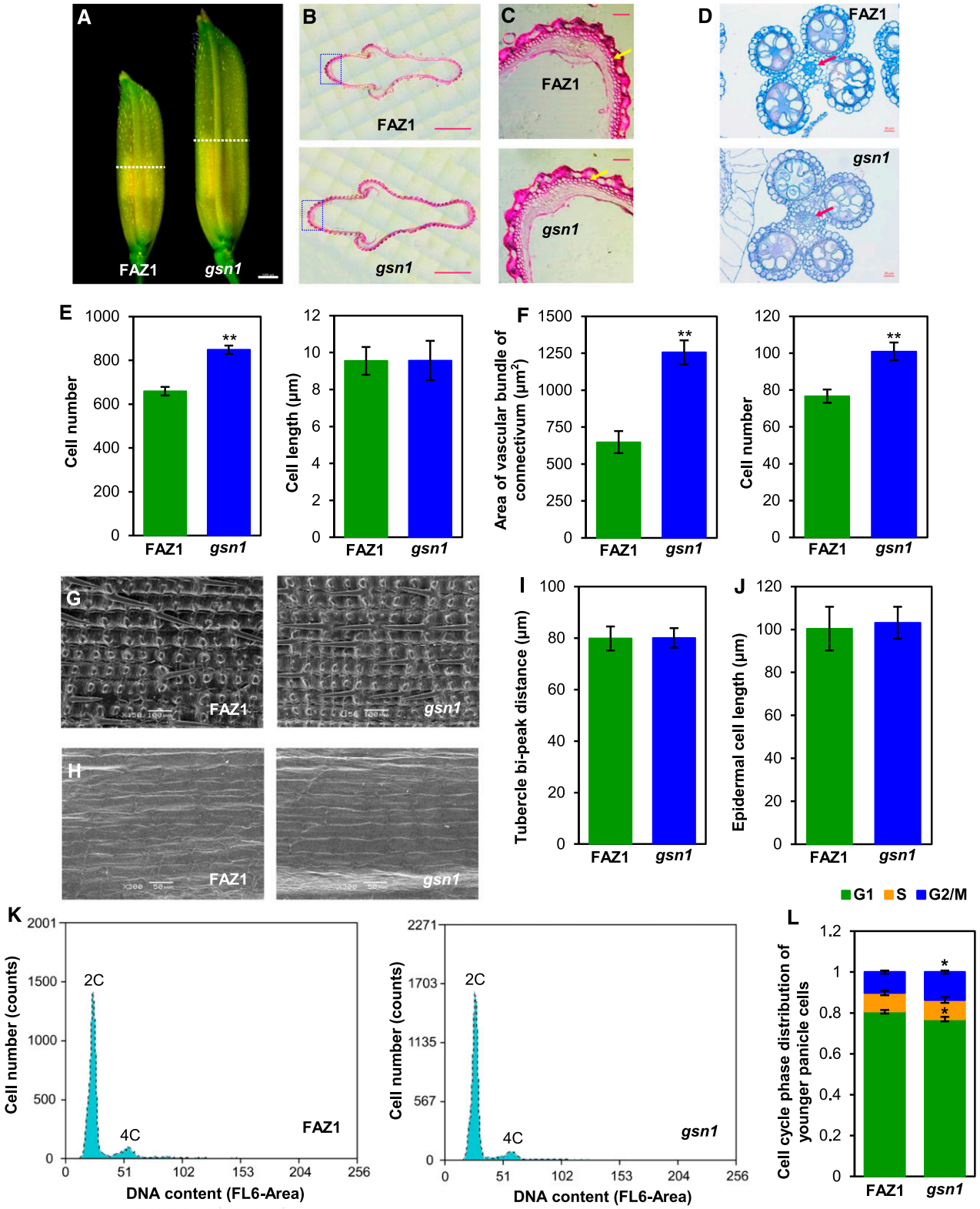

Figure 3. *GSN1* Influences Cell Proliferation Rather Than Cell Elongation to Control Organ Size.

(A) Spikelet hulls just before heading in FAZ1 and *gsn1*. The dotted line indicates the position of the cross-section shown in **(B)**. Bar = 1 mm.
(B) Cross sections of FAZ1 and *gsn1* spikelet hulls. Bar = 300 μm.

OsMPK6-Myc coimmunoprecipitated with GSN1-Flag instead of the negative control. These results further confirm that GSN1 interacts with OsMPK6 in vivo (Figure 5C). We then performed phosphorylation and dephosphorylation assays to determine whether GSN1 can dephosphorylate and inactivate OsMPK6 in vitro. GST-OsMPK6 protein expressed in *E. coli* and purified as substrate was primarily phosphorylated and activated by a constitutively active version of OsMKK4 (LOC_Os02g54600) known as MBP-OsMKK4^{CA} that carries the T238D and S244D mutations (Yang et al., 2001). We then used the activated GST-OsMPK6 in a dephosphorylation reaction with MBP-GSN1 and MBP-GSN1^{S146F}. The use of the phospho-p44/42 antibody specifically showed that GST-OsMPK6 can be activated in the T-E-Y motif of the activation loop by MBP-OsMKK4^{CA}, following inactivation by MBP-GSN1 rather than MBP-GSN1^{S146F}, which both exhibited a dosage effect (Figure 5D). We further characterized the T-E-Y motif of the activation loop in both the activated and inactivated forms of GST-OsMPK6 by mass spectrometry (Supplemental Figures 11A and 11B). Consistent with the results of the in vitro phosphorylation and dephosphorylation assays, the phosphorylation levels of OsMPK6 obviously increased in the younger panicles of *gsn1* and the repression lines of *GSN1* but markedly decreased in the overexpression lines (Supplemental Figure 12). These results confirm that GSN1 can interact with and inactivate OsMPK6 via dephosphorylation in vitro and in vivo.

GSN1 Acts as a Negative Regulator of the MAPK Cascade in Coordinating the Trade-off between Grain Number and Grain Size

Given that GSN1 associates with and dephosphorylates OsMPK6 and that OsMKK4 can interact with and activate OsMPK6 (Figure 5D; Supplemental Figure 11C), both of which are thought to act on the same cascade influencing rice grain size that depends on cell proliferation (Duan et al., 2014; Liu et al., 2015), we attempted to identify the components of the MAPK cascade that participate in panicle and spikelet development in rice, as well as the genetic association between *GSN1* and the MAPK signaling pathway. We therefore performed genome editing using CRISPR/Cas9 in the wild-type FAZ1 background. Unfortunately, we were not able to isolate the related loss-of-function mutants for *OsMPK6* due to embryo lethality, which is consistent with the results of a previous study (Yi et al., 2016); instead, we used gene knockdown mutants produced based on RNA interference (RNAi). We found that the *OsMPK6^{RNAi}* single mutant, which showed reduced expression of *OsMPK6*, had reduced grain size and increased grain number per panicle compared with the wild-type FAZ1, strongly suggesting that *OsMPK6* is a positive regulator of grain size and is required for panicle and spikelet development (Figures 6A, 6B, and 6G). In agreement with this notion, the downregulation of *OsMPK6* expression in the *gsn1/OsMPK6^{RNAi}* double mutant partially rescued the grain size and grain number per panicle phenotypes of *gsn1*, which indicates that the larger grains and sparser panicles in the *gsn1* mutant rely on *OsMPK6* and that there is a conclusive genetic association between *GSN1* and *OsMPK6* (Figures 6A, 6B, and 6G; Supplemental Figures 13A, 13B, and 14A). Furthermore, plants of the *OsMKK4* null mutant produced by CRISPR/Cas9 gene editing, *OsMKK4^{CRISPR}*, exhibited smaller grains and denser panicles than the wild type, which are very similar to the phenotypes observed in the *small grain1* mutants (Duan et al., 2014). In addition, the double mutant *gsn1/OsMKK4^{CRISPR}* perfectly rescued the mutant *gsn1* phenotypes by mimicking the grain size and grain number per panicle of FAZ1 (Figures 6C, 6D, and 6H; Supplemental Figures 13C, 13D, and 14B). Interestingly, overexpression of the constitutively active version of *OsMKK4* in FAZ1 resulted in plants with increased grain size and reduced grain number per panicle (Supplemental Figure 15). These results suggest that *OsMKK4* is a positive regulator of grain size but a negative regulator of grain number per panicle and that the phenotypes of the *gsn1* mutant that result from disordered cell proliferation and differentiation largely depend on *OsMKK4*. Considering the association of the phenotypes and protein characterization results between *OsMPK6* and *OsMKK4*, we hypothesized that the OsMKK4-OsMPK6 module, which participates in panicle and spikelet development, may be inactivated by GSN1.

In *Arabidopsis thaliana*, the proposed complete YODA (YDA)-MKK4/MKK5-MPK3/MPK6 cascade plays a critical role in specifying inflorescence architecture by promoting localized cell proliferation; the *yda* mutant has a tight, compact inflorescence, and YDA is an upstream regulator of MKK4/MKK5 during inflorescence development (Meng et al., 2012). The rice homolog of *YDA* has not yet been identified. We asked whether the rice homolog of the Arabidopsis *YDA* gene might coordinate the trade-off between grain size and grain number per panicle in rice and act upstream of the OsMKK4-OsMPK6 module. We searched the Phytozome database and found that *OsMKKK10* (LOC_Os04g47240) (Rao et al., 2010) shares high sequence similarity with Arabidopsis *YDA* and has an unknown function in rice. Therefore, we generated

Figure 3. (continued).

(C) Magnified views of the spikelet hull cross-sections boxed in **(B)**. Arrows show the outer parenchymal cell layer. Bar = 50 μm.
(D) Cross sections of FAZ1 and *gsn1* anthers. Arrows show the vascular bundle cells of the connectivum. Bar = 20 μm.
(E) Comparisons of cell numbers and average cell length in the outer parenchymal cell layers of FAZ1 and *gsn1* spikelet hulls (n = 10 views).
(F) Comparisons of the average area of the vascular bundles in the connectivum and cell numbers in the connectivum in FAZ1 and *gsn1* (n = 10 views).
(G) and **(H)** Scanning electron micrographs of the outer **(G)** and inner **(H)** surfaces of FAZ1 and *gsn1* spikelet hulls. Bars = 100 and 50 μm, respectively.
(I) Comparison of average tubercle bi-peak distance on the outer surfaces of the spikelet hulls between FAZ1 and *gsn1* (n = 10 grains).
(J) Comparison of inner epidermal cell length in FAZ1 and *gsn1* spikelet hulls (n = 10 grains).
(K) Flow cytometry analysis of young panicle (1–3 cm) cells in FAZ1 and *gsn1*. The tall and short peaks show 2c and 4c nuclei, respectively.
(L) Percentage comparison of the distribution of cells in different phases of the cell cycle in young spikelet cells (n = 10 pooled tissues, and three younger panicles from different plants per pool). The G1, S, and G2/M phases are shown in colored boxes. All numerical values are given as the mean ± SD. *$P < 0.05$ and **$P < 0.01$ compared with the wild type using Student's t test.

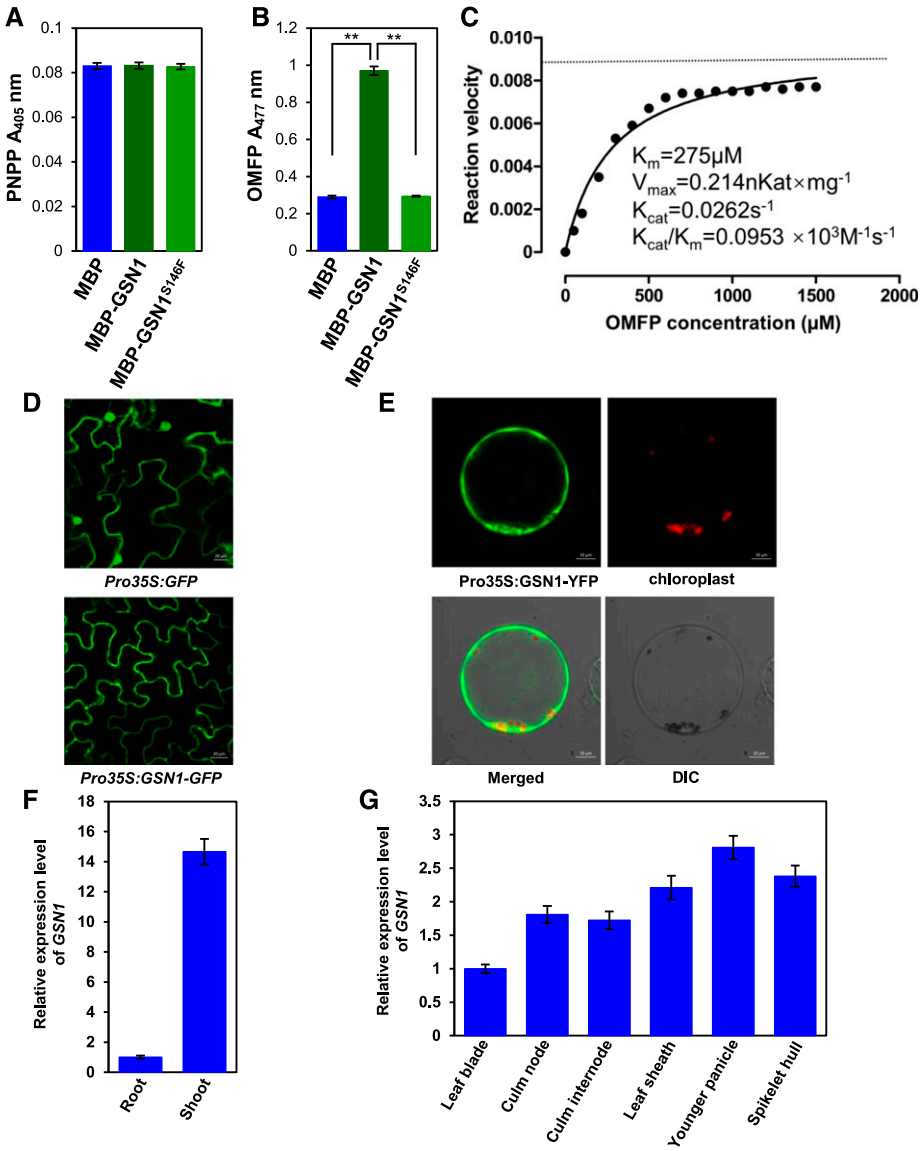

Figure 4. *GSN1* Encodes a Dual-Specificity Phosphatase with Dephosphorylation Activity That Localizes to the Cytoplasm.

(A) and **(B)** GSN1 specifically dephosphorylates the bulky polycyclic aryl phosphate OMFP but not PNPP. The enzymatic activity of GSN1 from FAZ1 and *gsn1* was examined using MBP fusion proteins expressed in *E. coli* using the substrates PNPP **(A)** and OMFP **(B)**. Dephosphorylated OMFP and PNPP levels were determined based on absorbance at 477 and 405 nm after the dephosphorylation reactions were complete (n = 10 independent dephosphorylation reactions). MBP protein was used as the negative control. Values are given as the mean ± SD. **P < 0.01 compared with the wild type and the negative control using Student's t test.

(C) Enzymatic characterization of GSN1 activity. The kinetic parameters K_m and V_{max} for GSN1 using OMFP as a substrate were calculated using GraphPad Prism 5 software.

(D) Subcellular localization of GSN1 in leaf epidermal cells of *N. benthamiana*. The *Pro35S:GFP* construct was used as the positive control and was distributed ubiquitously. Bar = 20 μm.

(E) GSN1 protein was shown to target the cytoplasm by transient expression analysis of GSN1-YFP in rice protoplasts. DIC, differential interference contrast. Bar = 2 μm.

(F) and **(G)** Relative expression levels of *GSN1* in various organs in the vegetative **(F)** and reproductive phase **(G)** determined by qRT-PCR (n = 3 pooled tissues, three plants per pool). Values are given as the mean ± SD. The *UBQ5* gene was used as an internal reference to normalize gene expression data.

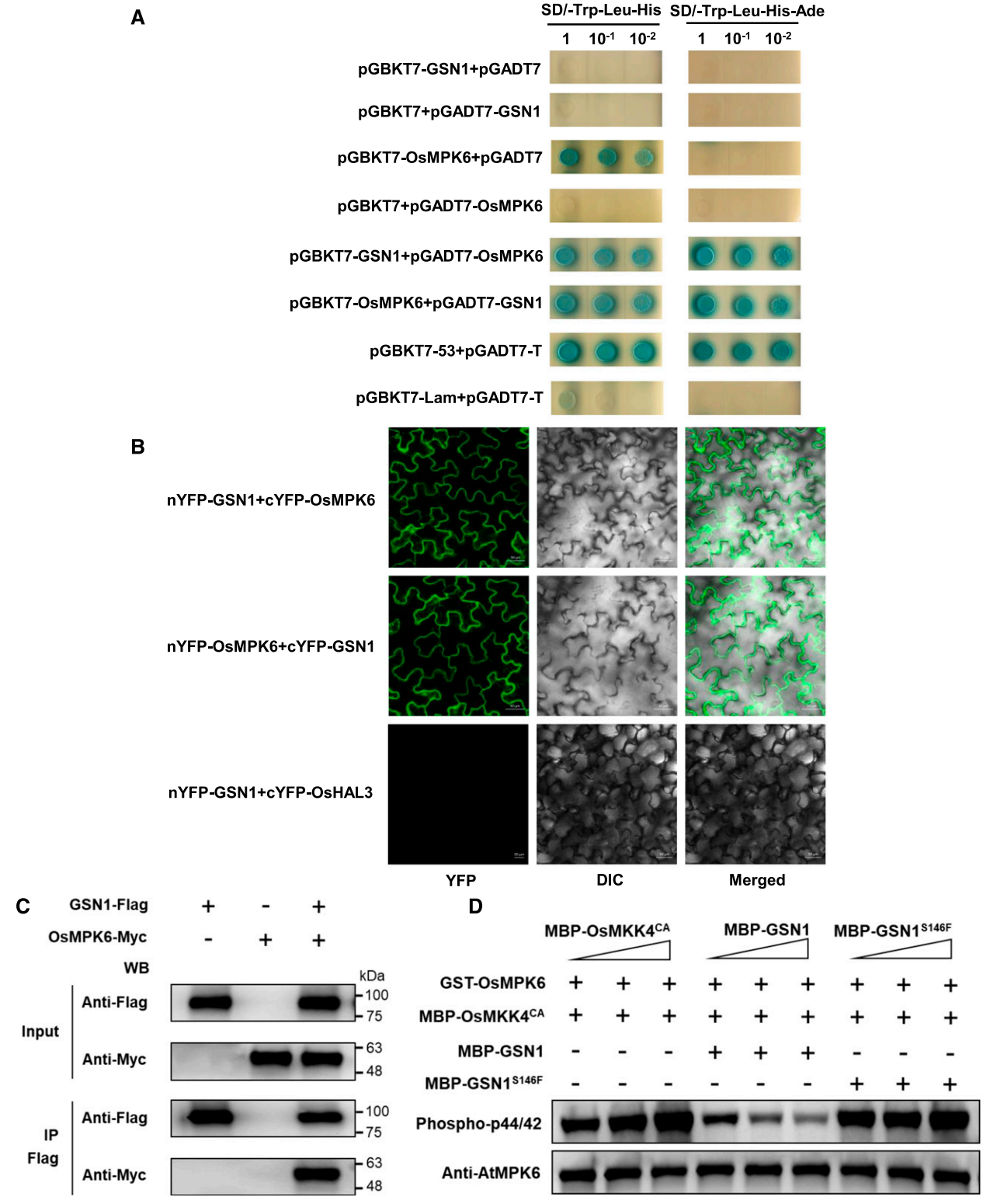

Figure 5. GSN1 Interacts with and Inactivates OsMPK6 via Specific Dephosphorylation.

(A) Yeast two-hybrid assays indicate that GSN1 interacts with OsMPK6. The yeast cells were cultured on SD/-Trp-Leu-His (medium without tryptophan, leucine, and histidine) or SD/-Trp-Leu-His-Ade (medium without tryptophan, leucine, histidine, and adenine) containing X-α-gal. pGBKT7 and pGADT7 are the bait and prey vectors, respectively.

OsMKKK10 single mutants using CRISPR/Cas9, from which the *OsMKKK10*^{CRISPR} null mutant was isolated and characterized. In line with our hypothesis, the loss-of-function mutant *OsMKKK10*^{CRISPR} had smaller grains but denser panicles with more grains per panicle than the wild type, which is analogous to the *OsMKK4*^{CRISPR} mutant, suggesting that *OsMKKK10* plays a conserved role in plant inflorescence development and is responsible for rice grain number per panicle and grain size and may act upstream of *OsMKK4* (Figures 6E, 6F, and 6I; Supplemental Figures 13E, 13F, and 14C). We also generated the *gsn1*/*OsMKKK10*^{CRISPR} double mutant and we found that it rescued the *gsn1* phenotypes, suggesting that the phenotypes observed in the *gsn1* mutant are also mostly dependent on *OsMKKK10* in rice and that this gene likely participates in panicle and spikelet formation in the combined *OsMKK4-OsMPK6* module regulated by *GSN1* (Figures 6E, 6F, and 6I; Supplemental Figures 13E, 13F, and 14C).

These results indicate that the reduced function of *OsMPK6* and the loss of function of *OsMKK4* and *OsMKKK10* can all rescue the *gsn1* panicle and spikelet phenotypes to different extents and together contribute to panicle and spikelet development, which is consistent with the strong expression of *OsMPK6*, *OsMKK4*, and *OsMKKK10* in young panicles and spikelet hulls (Supplemental Figures 10I to 10K). Finally, we assayed the phosphorylation level of OsMPK6 in young panicles in different transgenic plants and found that suppression of *OsMPK6*, *OsMKK4*, and *OsMKKK10* expression rescued the phosphorylation level of OsMPK6 in *gsn1* (Supplemental Figure 16). These results suggest that the phosphorylation status of OsMPK6, which is precisely regulated by the GSN1-MAPK module, is pivotal for panicle development in rice. In summary, we hypothesize that *OsMPK6*, *OsMKK4*, and *OsMKKK10* act in a common signaling pathway and that the proposed OsMKKK10-OsMKK4-OsMPK6 cascade, which is inactivated by GSN1, is responsible for specifying the trade-off between grain number per panicle and grain size. This trade-off results from the coordination between cell differentiation in the panicle and localized cell proliferation in the spikelet.

DISCUSSION

Both grain number per panicle and grain size are essential agronomic traits in rice that strongly affect grain yield. It is well known that a panicle with larger grains always has reduced grain number and that spatiotemporally, the determination of panicle identity and spikelet number per panicle occurs prior to the complete development of the spikelet. This is true because of the constraint of intrinsic programs, although a larger panicle could simultaneously have both larger grains and grain number (Hu et al., 2015; Si et al., 2016) or have both fixed grain size and more grains when properly modified (Ashikari et al., 2005; Wu et al., 2016; Huo et al., 2017). Several genes involved in determining grain number and grain size have been characterized, which always exhibit a preference and separate these two traits. Nevertheless, the inherent correlation between grain size and grain number per panicle tends to be ignored, although these two traits have different and interactive developmental processes. It is well known that there is a negative correlation between seed number and seed size in many plant species, which plays a central evolutionary role (Sadras, 2007). However, the genetic basis for coordinating the trade-off between grain number per panicle and grain size in rice remains largely unknown.

In this study, we first determined that *GSN1* is a negative regulator of grain size but a positive regulator of grain number per panicle, which specifically links these two traits through a conserved MAPK cascade. *GSN1* encodes a dual-specificity phosphatase that can inactivate OsMPK6 by dephosphorylation, and the phosphorylation level of OsMPK6 is excessively enhanced in *gsn1* (Figure 5; Supplemental Figures 12 and 16). GSN1 is localized to the cytoplasm and is mainly expressed in younger panicles and spikelets (Figure 4). Reduced expression of *GSN1* resulted in larger but fewer grains per panicle, whereas its upregulation increased grain number per panicle but reduced grain size (Figure 2; Supplemental Figure 2). Molecular evidence revealed that the expression of most of the downstream cell division-related genes was largely increased in the *gsn1* mutant compared with FAZ1, whereas genes responsible for primordium differentiation and grain number formation, such as *DENSE AND ERECT PANICLE1*, *Grain number 1a*/*CYTOKININ OXIDASE2* (*Gn1a*/*OsCKX2*), and *LAX PANICLE1*, were either significantly up- or downregulated in the *gsn1* mutant (Supplemental Figure 7). Interestingly, loss of function of *OsMKKK10* or *OsMKK4*, and reduced expression of *OsMPK6*, rescued the larger grain size and reduced grain number phenotypes in *gsn1* (Figure 6; Supplemental Figures 13 and 14), supporting the hypothesis that *GSN1* negatively regulates the *OsMKKK10-OsMKK4-OsMPK6* cascade. Although the proposed YDA-MKK4/MKK5-MPK3/MPK6 cascade in Arabidopsis has been shown to participate in inflorescence development (Meng et al., 2012), we found that the rice OsMKKK10-OsMKK4-OsMPK6 cascade, which is inactivated by GSN1, plays a distinct role in specifying the trade-off between grain number per panicle and grain size.

Figure 5. (continued).

(B) GSN1 associates with OsMPK6, as shown by BiFC assays in *N. benthamiana* leaf cells. GSN1 and OsMPK6 were both fused to the N-terminal fragment of YFP (nYFP) and the C-terminal fragment of YFP (cYFP). nYFP-GSN1 and cYFP-OsMPK6, or cYFP-GSN1 and nYFP-OsMPK6 were then coexpressed in *N. benthamiana* leaves. The nYFP-GSN1 and cYFP-OsHAL3 fusion proteins were used as negative controls.

(C) Coimmunoprecipitation assays indicate that GSN1 interacts with OsMPK6 in planta. *Pro35S:GSN1-Flag* and *Pro35S:OsMPK6-Myc* fusions were coexpressed in *N. benthamiana* leaves. Proteins were extracted (Input) and immunoprecipitated (IP) with Flag beads. The immunoblot (WB for protein gel blot) assays were performed using anti-Flag and anti-Myc antibodies.

(D) GSN1 dephosphorylates OsMPK6 in vitro. The MBP-GSN1, MBP-GSN1^{S146F}, MBP-OsMKK4^{CA}, and GST-OsMPK6 proteins were expressed in *E. coli* and purified using MBP and GST beads, respectively. The in vitro phosphorylation and dephosphorylation reactions were performed using the purified proteins. OsMPK6 phosphorylation was detected using the polyclonal antibody phospho-p44/42. The loading control was blotted using the anti-AtMPK6 antibody against Arabidopsis MPK6.

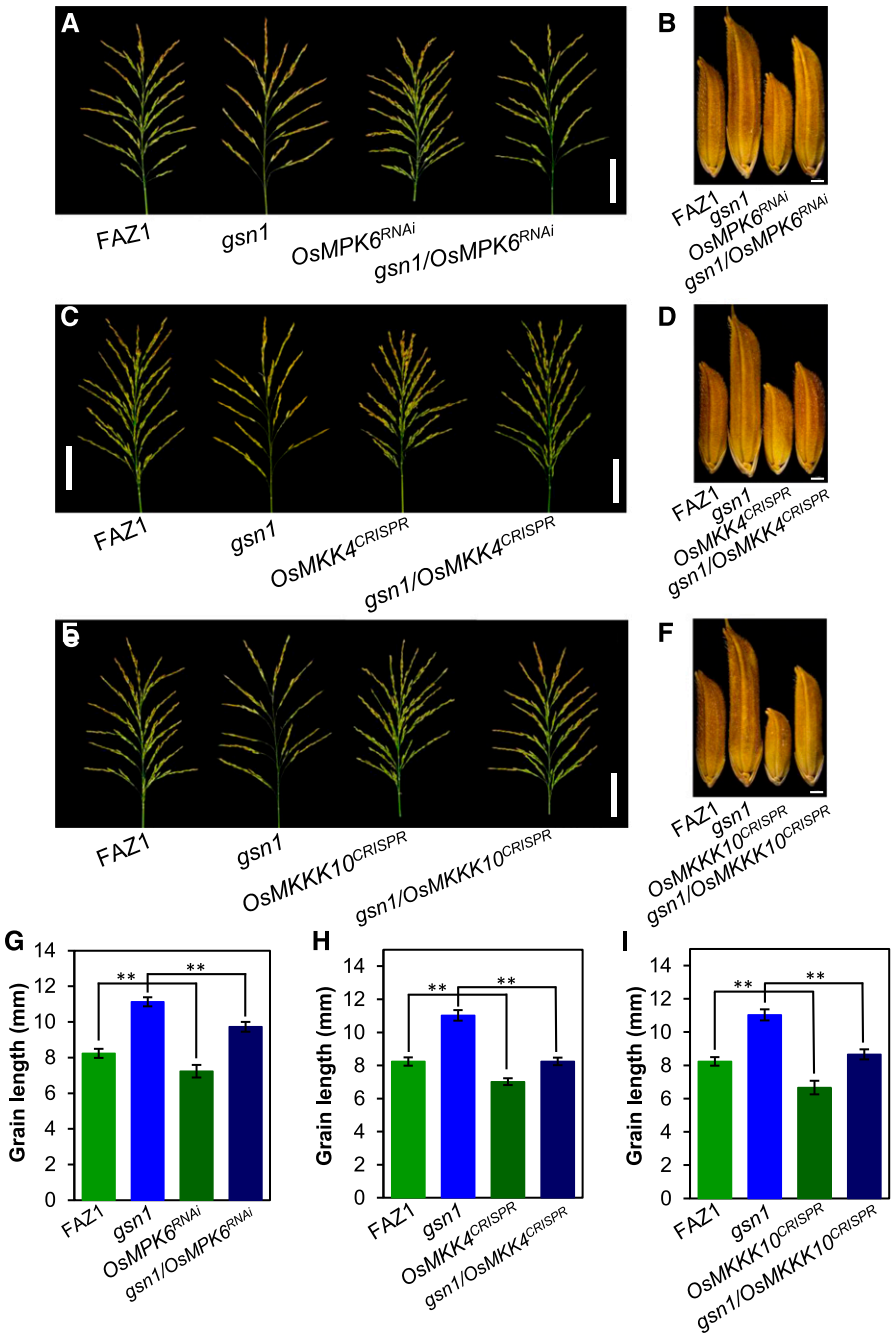

Figure 6. *GSN1* Is a Negative Regulator of the MAPK Cascade Signaling Pathway in Rice.

(A) and **(B)** Panicle **(A)** and grain **(B)** morphology in FAZ1, *gsn1*, *OsMPK6*^{RNAi}, and *gsn1*/*OsMPK6*^{RNAi} double mutant plants. Bars = 5 cm and 1 mm, respectively.

(C) and **(D)** Panicle **(C)** and grain **(D)** morphology in FAZ1, *gsn1*, *OsMKK4*^{CRISPR}, and the *gsn1*/*OsMKK4*^{CRISPR} double mutant. Bars = 5 cm and 1 mm, respectively.

(E) and **(F)** Panicle **(E)** and grain **(F)** morphology in FAZ1, *gsn1*, *OsMKKK10*^{CRISPR}, and the *gsn1*/*OsMKKK10*^{CRISPR} double mutant. Bars = 5 cm and 1 mm, respectively.

(G) Comparison of average grain length in FAZ1, *gsn1*, *OsMPK6*^{RNAi}, and the *gsn1*/*OsMPK6*^{RNAi} double mutant (n = 15 plants).

(H) Comparison of average grain length in FAZ1, *gsn1*, *OsMKK4*^{CRISPR}, and the *gsn1*/*OsMKK4*^{CRISPR} double mutant (n = 15 plants).

(I) Comparison of average grain length in FAZ1, *gsn1*, *OsMKKK10*^{CRISPR}, and the *gsn1*/*OsMKKK10*^{CRISPR} double mutant (n = 15 plants).

Values in **(G)** to **(I)** are given as the mean ± SD. **P < 0.01 compared with FAZ1 and *gsn1* using Student's *t* test.

Taken together, we proposed a working model for the role of the GSN1-MAPK module in the trade-off between grain number per panicle and grain size. After sensing panicle cell-specific communication signaling molecules (e.g., peptide ligands), unknown receptors, including receptor-like protein kinases, activate the OsMKKK10-OsMKK4-OsMPK6 cascade directly or through unknown mediators. The activated OsMKKK10-OsMKK4-OsMPK6 cascade sequentially phosphorylates its unidentified downstream substrates, which ultimately determine cell differentiation in the panicle primordia and cell proliferation in the spikelet and confer grain number per panicle and grain size at the young panicle developmental stage. The spatiotemporally activated GSN1 protein acts like a molecular brake to negatively regulate the OsMKKK10-OsMKK4-OsMPK6 cascade and precisely inactivates OsMPK6, which then represses the phosphorylation of substrates. Hence, the signaling output of the integrated GSN1-MAPK module coordinates the trade-off between grain number per panicle and grain size, ultimately determining panicle architecture in rice (Figure 7).

MAPK cascades are highly conversed, pivotal signaling pathways in eukaryotes. Numerous studies have demonstrated the multiple roles of diverse, specific combinations of MAPK cascades in regulating cell growth or environmental stress responses (Widmann et al., 1999). Genes for MAPK cascade components are abundant in plants genomes and can form many distinct MKKK-MKK-MPK combinations. However, studies of plant MAPKs have mainly focused on their functions in immunity and stress responses, although MAPKs play essential roles in multiple developmental programs. For example, the perception of flagellin pathogen-associated molecular patterns by receptors leads to the activation of the MEKK1-MKK1/MKK2-MPK4 cascade, which represses cell death and immune responses in Arabidopsis (Rodriguez et al., 2010; Kong et al., 2012). In addition, in rice, the perception of chitin signals at the cell surface by the pathogen-associated molecular pattern receptor OsCERK1 triggers the rapid activation of MAPK cascade required for resistance to rice blast fungus (Wang et al., 2017). While the YODA-MKK4/MKK5-MPK3/MPK6 cascade also regulates stomatal development and patterning by coordinating cell differentiation in Arabidopsis (Wang et al., 2007; Lampard et al., 2008), the complete MAPK components and module that confer the specific developmental programs in rice are still largely unknown. In this study, the discovery of the proposed OsMKKK10-OsMKK4-OsMPK6 cascade, which coordinates the trade-off between seed number and seed size, provides important insights into plant inflorescence development. Furthermore, studies aimed at identifying negative regulators of MAPK cascades specifying plant developmental programs have rarely been performed. Here, we demonstrated that *GSN1* encodes a dual-specificity phosphatase that is a negative regulator of MAPK that specifically dephosphorylates OsMPK6 and inactivates the OsMKKK10-OsMKK4-OsMPK6 cascade in rice to regulate the trade-off between grain number per panicle and grain size. Reversible phosphorylation is an important regulatory mechanism that controls the activities of some proteins and determines the intensity and duration of MAPK signaling activation. Dual-specificity phosphatases are crucial negative regulators of MAPK cascades, and they specifically dephosphorylate both phosphotyrosine and phosphoserine/threonine residues within the activation motifs of MAPKs to trigger the inactivation of MAPK cascades. Notably, we found that GSN1 also interacts with and dephosphorylates OsMPK3 (LOC_Os03g17700), as does its homolog, OsMPK6, implying that GSN1 associates with other MAPKs to regulate diverse processes during rice development (Supplemental Figure 17). Therefore, the discovery of the proposed rice GSN1-MAPK module provides important insights into the precise regulation of MAPK cascades via a dual-specificity phosphatase to remodel plant inflorescence development.

The essential phytohormones brassinosteroid (BR) and cytokinin play vital roles in numerous developmental programs in plants. The *small grain1* and *dwarf and small grains1* rice mutants are relatively insensitive to BR and share several similar phenotypes with BR mutants, such as small grains and erect panicles and leaves, indicating that both *OsMPK6* and *OsMKK4* influence BR homeostasis and signaling (Duan et al., 2014; Liu et al., 2015). Consistent with this notion, we found that the *gsn1* mutant was hypersensitive to BR and that the expression levels of BR-related genes, including BR biosynthesis and signal transduction genes, were significantly elevated in the *gsn1* mutant, although the contents of BR and its precursor in younger panicles were essentially unchanged (Supplemental Figure 18). These results suggest that the loss of function of *GSN1* can trigger the BR response and that the maintenance of BR homeostasis is required for the functioning of the GSN1-MAPK module, which might confer plasticity in grain size in the rice panicle.

Interestingly, attenuation of the cytokinin metabolic enzyme Gn1a/OsCKX2 causes the accumulation of cytokinin and enhances cell proliferation in the meristem, resulting in a significant increase in grain number (Ashikari et al., 2005). We found that *Gn1a/OsCKX2* was significantly upregulated in *gsn1* compared with FAZ1 during young panicle developmental, but the expression of the cytokinin-activating gene *LOG* was dramatically reduced in this mutant (Kurakawa et al., 2007) (Supplemental Figure 7B). In agreement with this finding, the levels of several cytokinins and their biosynthetic intermediates were significantly reduced in the mutant (Supplemental Figure 19). Thus, we hypothesize that cytokinin activity is substantially attenuated in the *gsn1* panicle meristem, which contributes to its reduced grain number per panicle. These findings point to a potential association between the GSN1-MAPK module and phytohormone signaling in the determination of panicle architecture plasticity in rice.

Although an evolutionary understanding of the trade-off and plasticity between seed number and seed size is crucial for inflorescence remodeling and the improvement of grain yield, little is known about the molecular mechanisms behind the plasticity determining final inflorescence architecture in plants. Therefore, this study represents an initial step in dissecting the mechanism by which the GSN1-MAPK module coordinates the trade-off between grain number per panicle and grain size. Further identification of the components upstream and downstream of the GSN1-MAPK module will ultimately reveal the molecular mechanisms underlying the coordination of localized cell differentiation and proliferation, which contributes to the trade-off between grain number per panicle and grain size in rice.

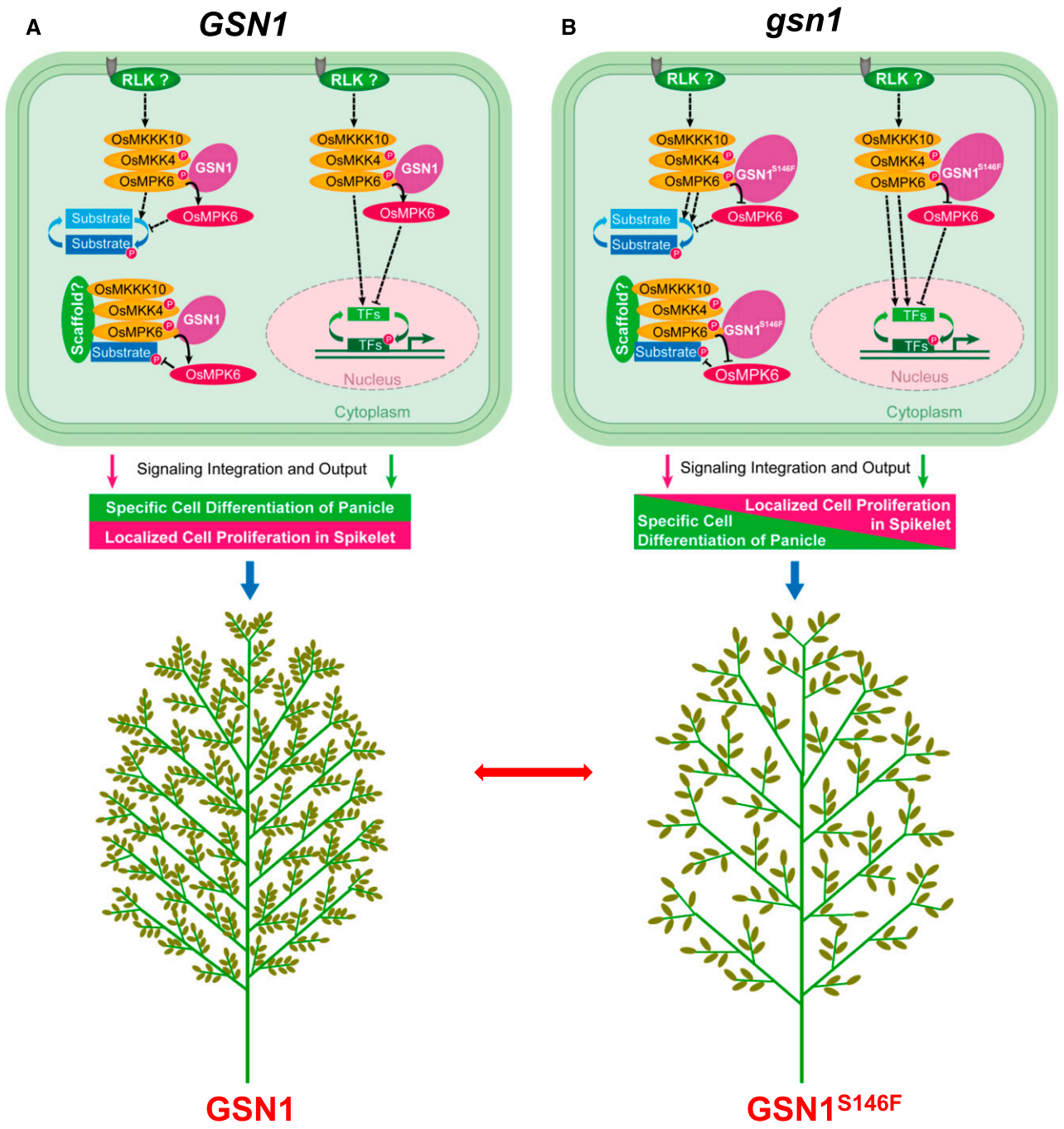

Figure 7. Proposed Working Model of the Role of the GSN1-MAPK Module in Determining Grain Number per Panicle and Grain Size in Rice.

(A) and **(B)** In young panicles at a specific developmental stage, after sensing panicle cell-specific communication signaling molecules, unknown receptor-like protein kinases activate the OsMKKK10-OsMKK4-OsMPK6 cascade through mediators or scaffold proteins. This cascade sequentially phosphorylates downstream, unidentified substrates that determine cell differentiation in the panicle primordia or cell proliferation in the spikelet.

(A) Spatiotemporally activated GSN1 protein acts as a molecular brake and precisely dephosphorylates OsMPK6 and then inactivates the OsMKKK10-OsMKK4-OsMPK6 cascade, which represses the phosphorylation of downstream substrates.

(B) The inactivation of GSN1 (GSN1^{S146F}) results in direct, durative activation of the OsMKKK10-OsMKK4-OsMPK6 cascade and excessive amplification of downstream signaling, which attenuates cell differentiation in the panicle primordia but increases cell proliferation in the spikelet. Hence, the signaling output of the integrated GSN1-MAPK module coordinates the trade-off between grain number per panicle and grain size, ultimately contributing to final panicle architecture in rice. Arrows with solid lines show associations that are supported by genetic or biochemical evidence. Arrows with dashed lines show the presumptive associations. Double lines represent durative activation signaling. Question marks indicate unidentified or unknown signaling components.

METHODS

Plant Materials and Growth Conditions

The *gsn1* mutant was isolated from EMS-treated seeds of the elite *indica* rice (*Oryza sativa*) variety, Fengaizhan-1 (FAZ1). The M1 *gsn1* mutant was crossed back to FAZ1 to produce M2 plants in an isogenic background. All rice plants were cultivated in experimental fields in Shanghai and Hainan, China under natural growth conditions.

Map-Based Cloning of *GSN1*

The *gsn1* mutant was crossed with the *japonica* variety, Zhonghua 11 (ZH11), and F1 plants were self-pollinated to generate an F2 mapping population. To fine-map the *GSN1* locus, new molecular markers were developed. *GSN1* was mapped to a 17.5-kb region on the short arm of chromosome 5, and DNA fragments from this region were amplified from genomic DNA from both *gsn1* and the wild type for further sequencing. The PCR primer sets used for gene amplification are shown in Supplemental Data Set 1.

Plasmid Construction and Plant Transformation

To produce the complementation construct pCAMBIA1300-g*GSN1*, the full-length genomic sequence of *GSN1* was amplified from the wild type and cloned into the plant binary vector pCAMBIA1300. A 2.5-kb DNA fragment upstream of the *GSN1* start codon was amplified from FAZ1 and cloned into the pCAMBIA1300-GUSplus vector to generate the plasmid *ProGSN1*:GUS. The artificial microRNA oligo sequences used for *GSN1* silencing were designed as previously described (Warthmann et al., 2008). To generate the overexpression constructs, the full-length coding sequence of *GSN1* was amplified from both FAZ1 and *gsn1* and cloned into plant binary vectors pCAMBIA1306 and pCAMBIA1301 under the control of the CaMV 35S promoter and the ubiquitin (UBI) promoter, respectively. To generate the *OsMPK6* RNAi lines, an *OsMPK6* DNA fragment from the FAZ1 wild-type line was amplified and cloned into pTCK303 to obtain the *OsMPK6* RNAi construct. To generate constitutively active OsMKK4^{CA}, the full-length coding sequence of *OsMKK4* harboring the T238D and S244D mutations was cloned into pCAMBIA1301. The gene editing constructs for *GSN1*, *OsMKKK10*, and *OsMKK4* via CRISPR/Cas9 were designed as previously described (Ma et al., 2015). *Agrobacterium tumefaciens*-mediated transformation of rice with strain EHA105 was performed as previously described (Hiei et al., 1994). The DNA constructs used in this study were generated using NEBuilder HiFi DNA Assembly Master Mix (NEB). All constructs were confirmed by sequencing. The PCR primer sets are given in Supplemental Data Set 1.

RNA Extraction and qRT-PCR

Total RNA was extracted from various plant tissues using Trizol reagent (Invitrogen). Reverse transcription was performed using ReverTra Ace qPCR RT Master Mix with gDNA Remover (Toyobo) from 500 ng total RNA. Quantitative RT-PCR analysis was performed on the ABI 7300 Real-Time PCR System with Fast Start Universal SYBR Green Master Mix with ROX (Roche), and the data were analyzed using the $2^{-\Delta\Delta CT}$ method. The *UBQ5* gene was used as the internal reference to normalize gene expression data. All analyses were repeated at least three times. PCR primer sets for gene amplification are given in Supplemental Data Set 1.

GUS Staining

GUS staining of *ProGSN1*:GUS transgenic plants was performed as described previously (Duan et al., 2014). The samples were stained in GUS staining buffer overnight at 37°C. The samples were then cleared in 75% ethanol to remove chlorophyll.

Histochemical Analysis

Plant materials were fixed in FAA (50% ethanol, 5% glacial acetic acid, and 5% formaldehyde) overnight at 4°C and dehydrated in a graded alcohol series. After fixing with xylene, the samples were embedded in Paraplast (Sigma-Aldrich) and sliced into 8-μm-thick sections with a rotary microtome (Leica). The prepared tissue sections were stained with safranin and observed under a light microscope (Leica).

Scanning Electron Microscopy

Spikelet hulls harvested just before heading were fixed in FAA (50% ethanol, 5% glacial acetic acid, and 5% formaldehyde) overnight at 4°C and dehydrated in a graded alcohol series. The samples were then dried in a critical point drier (Leica), gold sputter coated, and observed under a scanning electron microscope (Hitachi). Cell size and cell number were calculated using Image J software after scanning.

Nucleus Isolation and Assessment of Ploidy

Isolation of cell nuclei and assessment of ploidy were performed as described previously (Qi et al., 2012). Spikelet hulls of younger panicles were selected, soaked separately in nuclear isolation and staining solution (Beckman), and chopped with a sharp blade. After filtering the slurry through a 40-μm nylon filter, the suspension of nuclei was loaded into a Beckman Moflo for flow cytometric analysis, and the ploidy of approximate 10,000 nuclei was recorded for each test. The numbers of diploid and tetraploid nuclei were recorded, and the relative proportions of G1, S, and G2/M phase cells were calculated using FCS Express 4 software.

Subcellular Localization of GSN1

To determine the subcellular localization of GSN1, the *Pro35S:GSN1-GFP* DNA constructs were introduced into Agrobacterium strain GV3101 and infiltrated into the leaves of *Nicotiana benthamiana* plants. The *GSN1* fragment was inserted into the pA7-YFP plasmid and transformed into rice protoplasts. GFP fluorescence in leaf epidermal cells and YFP fluorescence in rice protoplasts were detected with an LSM 880 confocal laser-scanning microscope (Zeiss). The sequences of the PCR primers used for vector construction are given in Supplemental Data Set 1.

Yeast Two-Hybrid Assays

Yeast two-hybrid assays were performed with the Y2H Gold-Gal4 system (Clontech). DNA fragments containing the *GSN1*, *OsMPK6*, *OsMPK3*, and *OsMKK4* genes were inserted into the pGBKT7 and pGADT7 vectors to form the bait and prey constructs, respectively. The bait and prey constructs were transformed into yeast strain Y2H Gold according to the manufacturer's instructions (Clontech). The yeast cells were cultured on SD/-Trp-Leu-His or SD/-Trp-Leu-His-Ade medium containing X-α-gal at 30°C in the dark for 3 d. SD/-Trp-Leu-His is yeast culture medium without tryptophan, leucine, and histidine. SD/-Trp-Leu-His-Ade is culture medium without tryptophan, leucine, histidine, and adenine. The PCR primers used for yeast two-hybrid assays are given in Supplemental Data Set 1.

BiFC Assays

For the BiFC assays, the DNA fragments containing the *GSN1*, *OsMPK6*, *OsMPK3*, and *OsHAL3* genes were cloned into pCAMBIA1300S-YN and pCAMBIA1300S-YC to form the nYFP-protein and cYFP-protein constructs, respectively. Leaves of 5-week-old *N. benthamiana* plants were coinfiltrated with Agrobacterium strain GV3101 carrying the two constructs. The plants were grown in the dark for 48 h after infiltration, and BiFC fluorescence or protein localization fluorescence signals were then

observed using an LSM 880 confocal laser-scanning microscope (Zeiss). PCR primers used for BiFC are given in Supplemental Data Set 1.

Coimmunoprecipitation

The DNA fragment carrying *GSN1* was cloned into the pCAMBIA1306-Flag (3x) plasmid to produce the *Pro35S:GSN1-Flag* vector. The *OsMPK6* DNA fragment was cloned into pCAMBIA1301-Myc (7x)-His (6x) to generate the *Pro35S:OsMPK6-Myc* vector. The *Pro35S:GSN1-Flag* and *Pro35S:OsMPK6-Myc* constructs in Agrobacterium strain GV3101 were transiently coexpressed in *N. benthamiana* leaf cells following agroinfiltration. Protein extraction and immunoblot analyses were performed as previously described (Lee et al., 2012). The immunoblot (WB for protein gel blot) assays were performed using anti-Flag (Cell Signaling Technology; 14793) and anti-Myc (Cell Signaling Technology; 2276) antibodies at 1:1000 dilution. The PCR primers used for coimmunoprecipitation are given in Supplemental Data Set 1.

Protein Expression

The coding sequences of *GSN1*, *OsMKK4*, and their mutated versions were inserted into the pMAL-c5x vector. The coding regions of *OsMPK6* and *OsMPK3* were cloned into the pGEX-4T-2 vector. The recombinant pMAL-c5x and pGEX-4T-2 vectors were then transformed into Rossetta-gami (DE3) pLysS competent cells and cultured to produce fusion proteins. Amylose resin (NEB) and glutathione-agarose 4B (GE Healthcare) were used for fusion protein purification. The sequences of PCR primers used for protein expression are given in Supplemental Data Set 1.

Phosphatase Activity Assay

Phosphatase activity assays were performed as described previously (Lee et al., 2008). To analyze the activity of the dual-specificity phosphatase, OMFP (Sigma-Aldrich) and PNPP (Thermo Fisher) were used as substrates. The phosphatase activity of GSN1 or GSN1^{S146F} at various enzyme concentrations (0, 10, 20, 30, 40, 50, 60, 80, and 100 μg) was measured in 200-μL reactions containing phosphatase buffer (50 mM Tris-HCl, pH 8.0, 15 mM NaCl, and 1 mM EDTA) and 500 μM OMFP or PNPP, and the mixtures were incubated at 30°C for 1 h. Also, a series of OMFP concentrations (50, 100, 200, 300, 400, 500, 600, 700, 800, and 1000 μM) was prepared to analyze enzyme activity kinetics with the same amount of phosphatase at different time points (10, 30, 45, 60, 90, 120, 150, 180, 210, 240, 270, and 300 min). The amounts of dephosphorylated OMFP and PNPP were recorded based on the absorbance at 477 and 405 nm, respectively, after the dephosphorylation reaction. The kinetic parameters K_m and V_{max} for GSN1 were determined using OMFP as substrate and calculated using GraphPad Prism 5 software.

In Vitro Dephosphorylation Assays

The purified fusion proteins MBP-GSN1, MBP-GSN1^{S146F}, MBP-OsMKK4^{CA}, GST-OsMPK6, and GST-OsMPK3 were used in the dephosphorylation assays. Purified MBP-OsMKK4^{CA} was mixed with recombinant GST-OsMPK6 and GST-OsMPK3 at a 1:3 ratio in kinase buffer (25 mM Tris-HCl, pH 7.5, 5 mM β-glycerolphosphate, 2 mM DTT, 10 mM $MgCl_2$, and 200 μM ATP) and incubated at 30°C for 30 min. The reaction mixture was then desalted to separate free ATP. To dephosphorylate the fusion proteins GST-OsMPK6 and GST-OsMPK3, the recombinant MBP-GSN1 and MBP-GSN1^{S146F} proteins were mixed separately with phosphorylated GST-OsMPK6 and GST-OsMPK3 protein at a 1:4 ratio and incubated at 30°C for 30 min. The reaction was terminated by the addition of concentrated SDS-PAGE sample buffer, followed by boiling for 5 min. Phosphorylated GST-OsMPK6 and GST-OsMPK3 were visualized by immunoblot analysis using the polyclonal antibody phospho-p44/42 at 1:2000 dilution (Cell Signaling Technology; 9101), which specifically recognizes the dual-phosphorylated T-E-Y motif of the phosphorylated GST-OsMPK6 and GST-OsMPK3. The loading control was probed using anti-AtMPK6 (Sigma-Aldrich; A7104) and anti-AtMPK3 (Sigma-Aldrich; M8318) antibodies against Arabidopsis MPK6 and MPK3, respectively, at 1:2000 dilution.

Mass Spectrometry Analysis

The proteins from the phosphorylation and dephosphorylation assays were reduced with 10 mM DTT and alkylated with 50 mM iodoacetamide. In-solution digestion was performed using sequencing-grade modified trypsin (Promega) at 37°C overnight. The tryptic peptides were acidated with a final concentration of 0.5 to 1% trifluoroacetic acid. For mass spectrometry analysis, the peptides were separated via a 90 min gradient elution at a flow rate 0.22 μL/min with the EASY-nLC 1000 HPLC system (Thermo Scientific), which was directly interfaced with a Q Exactive mass spectrometer (Thermo Scientific). The mobile phase consisted of 0.1% formic acid, and the mobile phase consisted of acetonitrile with 0.1% formic acid. The Q Exactive mass spectrometer was operated in the data-dependent acquisition mode using Xcalibur 2.2 SP1 software. The MS/MS spectra from each run were searched against the target sequence using the Sequest HT and phosphoRS 3.0 modules in Proteome Discoverer software PD1.4 (Thermo Scientific), which followed these criteria: full tryptic specificity was required; two missing cleavages were allowed; carbamidomethylation were set to fixed modifications; the oxidation was set to dynamic modification; precursor mass tolerances were set to 10 ppm; and the fragment mass tolerance was set to 0.02 D. The peptide false discovery rate < 1% was set using percolator in PD1.4.

Accession Numbers

Sequence data from this article can be found in the GenBank/EMBL libraries under the following accession numbers: *GSN1*, LOC_Os05g02500; *OsMPK6*, LOC_Os06g06090; *OsMPK3*, LOC_Os03g17700; *OsMKK4*, LOC_Os02g54600; and *OsMKKK10*, LOC_Os04g47240.

Supplemental Data

Supplemental Figure 1. *GSN1* is required for fertility in rice.

Supplemental Figure 2. Panicle phenotypes in transgenic RNA interference *GSN1^{RNAi}* lines and *ProUBI:GSN1* overexpression lines.

Supplemental Figure 3. Phenotypic characterization of 95-22 and the nearly isogenic line for *gsn1*, NIL(*gsn1*).

Supplemental Figure 4. Suppression of *GSN1* in ZH11 results in larger grains and sparser panicles.

Supplemental Figure 5. *GSN1^{S146F}* has a dominant-negative effect on panicle development in ZH11.

Supplemental Figure 6. Overexpression of *GSN1* in ZH11 results in smaller grains and denser panicles.

Supplemental Figure 7. Expression of cell cycle-related genes in young panicles (0.5–2 cm) of FAZ1 and *gsn1*.

Supplemental Figure 8. Overexpression of *GSN1* decreases cell proliferation rather than cell size to control grain length in FAZ1.

Supplemental Figure 9. Repression of *GSN1* increases cell proliferation rather than cell expansion to control grain length in ZH11.

Supplemental Figure 10. GUS staining showing *GSN1* expression in different tissues of *ProGSN1:GUS* transgenic rice plants.

Supplemental Figure 11. GSN1 specifically interacts with and inactivates OsMPK6 and not OsMKK4, but OsMPK6 interacts with OsMKK4.

Supplemental Figure 12. GSN1 dephosphorylates OsMPK6 in vivo.

Supplemental Figure 13. The reduced expression of *OsMPK6* or the loss of function of *OsMKK4* or *OsMKKK10* rescues the *gsn1* phenotypes.

Supplemental Figure 14. Confirmation of the *OsMPK6*^{RNAi}, *OsMKK4*^{CRISPR}, and *OsMKKK10*^{CRISPR} CRISPR/Cas9 transgenic lines.

Supplemental Figure 15. Overexpression of the constitutively active version of *OsMKK4*, *ProUBI:OsMKK4*^{CA}, specifically increases grain size in rice.

Supplemental Figure 16. Suppression of *OsMPK6*, *OsMKK4*, and *OsMKKK10* rescues the phosphorylation level of OsMPK6 in *gsn1*.

Supplemental Figure 17. GSN1 interacts with and dephosphorylates OsMPK3.

Supplemental Figure 18. The *gsn1* mutant is hypersensitive to BR, and *GSN1* influences BR signaling.

Supplemental Figure 19. *GSN1* is associated with the maintenance of cytokinin homeostasis during panicle development in rice.

Supplemental Data Set 1. Primers used in this study.

ACKNOWLEDGMENTS

We thank Min Shi (Institute of Plant Physiology and Ecology, SIBS, CAS) for technical support with the transgenic assay. We thank Xiaoshu Gao, Xiaoyan Gao, Zhiping Zhang, Jiqin Li, and Wenfang Zhao (Institute of Plant Physiology and Ecology, SIBS, CAS) for technical support. We thank Jian Zhang (China National Rice Research Institute) and Kang Chong (Institute of Botany, CAS) for donating the plasmids. This work was supported by grants from the Chinese Academy of Sciences (XDA08010102, QYZDY-SSW-SMC023, and XDPB0404), the National Natural Science Foundation of China (31788103), the Ministry of Science and Technology of China (2016YFD0100902), and CAS-Croucher Funding Scheme for Joint Laboratories.

AUTHOR CONTRIBUTIONS

H.-X.L., J.-X.S., and T.G. designed the study. T.G., K.C., N.-Q.D., C.-L.S., W.-W.Y., J.-P.G., J.-X.S., and H.-X.L. performed the experiments. T.G. and H.-X.L. analyzed the data and wrote the article.

Received December 19, 2017; revised February 12, 2018; accepted March 27, 2018; published March 27, 2018.

REFERENCES

Ashikari, M., Sakakibara, H., Lin, S., Yamamoto, T., Takashi, T., Nishimura, A., Angeles, E.R., Qian, Q., Kitano, H., and Matsuoka, M. (2005). Cytokinin oxidase regulates rice grain production. Science **309:** 741–745.

Bartels, S., González Besteiro, M.A., Lang, D., and Ulm, R. (2010). Emerging functions for plant MAP kinase phosphatases. Trends Plant Sci. **15:** 322–329.

Duan, P., Rao, Y., Zeng, D., Yang, Y., Xu, R., Zhang, B., Dong, G., Qian, Q., and Li, Y. (2014). SMALL GRAIN 1, which encodes a mitogen-activated protein kinase kinase 4, influences grain size in rice. Plant J. **77:** 547–557.

Hiei, Y., Ohta, S., Komari, T., and Kumashiro, T. (1994). Efficient transformation of rice (*Oryza sativa* L.) mediated by Agrobacterium and sequence analysis of the boundaries of the T-DNA. Plant J. **6:** 271–282.

Hu, J., et al. (2015). A rare allele of GS2 enhances grain size and grain yield in rice. Mol. Plant **8:** 1455–1465.

Huang, X., Qian, Q., Liu, Z., Sun, H., He, S., Luo, D., Xia, G., Chu, C., Li, J., and Fu, X. (2009). Natural variation at the DEP1 locus enhances grain yield in rice. Nat. Genet. **41:** 494–497.

Huo, X., Wu, S., Zhu, Z., Liu, F., Fu, Y., Cai, H., Sun, X., Gu, P., Xie, D., Tan, L., and Sun, C. (2017). NOG1 increases grain production in rice. Nat. Commun. **8:** 1497.

Kong, Q., Qu, N., Gao, M., Zhang, Z., Ding, X., Yang, F., Li, Y., Dong, O.X., Chen, S., Li, X., and Zhang, Y. (2012). The MEKK1-MKK1/MKK2-MPK4 kinase cascade negatively regulates immunity mediated by a mitogen-activated protein kinase kinase kinase in Arabidopsis. Plant Cell **24:** 2225–2236.

Kurakawa, T., Ueda, N., Maekawa, M., Kobayashi, K., Kojima, M., Nagato, Y., Sakakibara, H., and Kyozuka, J. (2007). Direct control of shoot meristem activity by a cytokinin-activating enzyme. Nature **445:** 652–655.

Lampard, G.R., Macalister, C.A., and Bergmann, D.C. (2008). Arabidopsis stomatal initiation is controlled by MAPK-mediated regulation of the bHLH SPEECHLESS. Science **322:** 1113–1116.

Lee, J.S., Kuroha, T., Hnilova, M., Khatayevich, D., Kanaoka, M.M., McAbee, J.M., Sarikaya, M., Tamerler, C., and Torii, K.U. (2012). Direct interaction of ligand-receptor pairs specifying stomatal patterning. Genes Dev. **26:** 126–136.

Lee, K., Song, E.H., Kim, H.S., Yoo, J.H., Han, H.J., Jung, M.S., Lee, S.M., Kim, K.E., Kim, M.C., Cho, M.J., and Chung, W.S. (2008). Regulation of MAPK phosphatase 1 (AtMKP1) by calmodulin in Arabidopsis. J. Biol. Chem. **283:** 23581–23588.

Li, Y., Fan, C., Xing, Y., Jiang, Y., Luo, L., Sun, L., Shao, D., Xu, C., Li, X., Xiao, J., He, Y., and Zhang, Q. (2011). Natural variation in GS5 plays an important role in regulating grain size and yield in rice. Nat. Genet. **43:** 1266–1269.

Liu, S., Hua, L., Dong, S., Chen, H., Zhu, X., Jiang, J., Zhang, F., Li, Y., Fang, X., and Chen, F. (2015). OsMAPK6, a mitogen-activated protein kinase, influences rice grain size and biomass production. Plant J. **84:** 672–681.

Luan, S. (2003). Protein phosphatases in plants. Annu. Rev. Plant Biol. **54:** 63–92.

Ma, X., et al. (2015). A robust CRISPR/Cas9 system for convenient, high-efficiency multiplex genome editing in monocot and dicot plants. Mol. Plant **8:** 1274–1284.

Mao, H., Sun, S., Yao, J., Wang, C., Yu, S., Xu, C., Li, X., and Zhang, Q. (2010). Linking differential domain functions of the GS3 protein to natural variation of grain size in rice. Proc. Natl. Acad. Sci. USA **107:** 19579–19584.

Meng, X., and Zhang, S. (2013). MAPK cascades in plant disease resistance signaling. Annu. Rev. Phytopathol. **51:** 245–266.

Meng, X., Wang, H., He, Y., Liu, Y., Walker, J.C., Torii, K.U., and Zhang, S. (2012). A MAPK cascade downstream of ERECTA receptor-like protein kinase regulates Arabidopsis inflorescence architecture by promoting localized cell proliferation. Plant Cell **24:** 4948–4960.

Oikawa, T., and Kyozuka, J. (2009). Two-step regulation of LAX PANICLE1 protein accumulation in axillary meristem formation in rice. Plant Cell **21:** 1095–1108.

Qi, P., Lin, Y.S., Song, X.J., Shen, J.B., Huang, W., Shan, J.X., Zhu, M.Z., Jiang, L., Gao, J.P., and Lin, H.X. (2012). The novel quantitative trait locus GL3.1 controls rice grain size and yield by regulating Cyclin-T1;3. Cell Res. **22:** 1666–1680.

Rao, K.P., Richa, T., Kumar, K., Raghuram, B., and Sinha, A.K. (2010). In silico analysis reveals 75 members of mitogen-activated protein kinase kinase kinase gene family in rice. DNA Res. **17:** 139–153.

Reyna, N.S., and Yang, Y. (2006). Molecular analysis of the rice MAP kinase gene family in relation to Magnaporthe grisea infection. Mol. Plant Microbe Interact. **19:** 530–540.

Rodriguez, M.C., Petersen, M., and Mundy, J. (2010). Mitogen-activated protein kinase signaling in plants. Annu. Rev. Plant Biol. **61:** 621–649.

Sadras, V.O. (2007). Evolutionary aspects of the trade-off between seed size and number in crops. Field Crops Res. **100:** 125–138.

Si, L., et al. (2016). OsSPL13 controls grain size in cultivated rice. Nat. Genet. **48:** 447–456.

Song, X.J., Huang, W., Shi, M., Zhu, M.Z., and Lin, H.X. (2007). A QTL for rice grain width and weight encodes a previously unknown RING-type E3 ubiquitin ligase. Nat. Genet. **39:** 623–630.

Su, L., Shan, J.X., Gao, J.P., and Lin, H.X. (2016). OsHAL3, a blue light-responsive protein, interacts with the floral regulator Hd1 to activate flowering in rice. Mol. Plant **9:** 233–244.

Wang, C., Wang, G., Zhang, C., Zhu, P., Dai, H., Yu, N., He, Z., Xu, L., and Wang, E. (2017). OsCERK1-mediated chitin perception and immune signaling requires receptor-like cytoplasmic kinase 185 to activate an MAPK cascade in rice. Mol. Plant **10:** 619–633.

Wang, H., Ngwenyama, N., Liu, Y., Walker, J.C., and Zhang, S. (2007). Stomatal development and patterning are regulated by environmentally responsive mitogen-activated protein kinases in Arabidopsis. Plant Cell **19:** 63–73.

Warthmann, N., Chen, H., Ossowski, S., Weigel, D., and Hervé, P. (2008). Highly specific gene silencing by artificial miRNAs in rice. PLoS One **3:** e1829.

Widmann, C., Gibson, S., Jarpe, M.B., and Johnson, G.L. (1999). Mitogen-activated protein kinase: conservation of a three-kinase module from yeast to human. Physiol. Rev. **79:** 143–180.

Wu, Y., Wang, Y., Mi, X.F., Shan, J.X., Li, X.M., Xu, J.L., and Lin, H.X. (2016). The QTL GNP1 encodes GA20ox1, which increases grain number and yield by increasing cytokinin activity in rice panicle meristems. PLoS Genet. **12:** e1006386.

Xing, Y., and Zhang, Q. (2010). Genetic and molecular bases of rice yield. Annu. Rev. Plant Biol. **61:** 421–442.

Xu, J., and Zhang, S. (2015). Mitogen-activated protein kinase cascades in signaling plant growth and development. Trends Plant Sci. **20:** 56–64.

Yang, K.Y., Liu, Y., and Zhang, S. (2001). Activation of a mitogen-activated protein kinase pathway is involved in disease resistance in tobacco. Proc. Natl. Acad. Sci. USA **98:** 741–746.

Yi, J., Lee, Y.S., Lee, D.Y., Cho, M.H., Jeon, J.S., and An, G. (2016). OsMPK6 plays a critical role in cell differentiation during early embryogenesis in *Oryza sativa*. J. Exp. Bot. **67:** 2425–2437.

Yoo, J.H., et al. (2004). Regulation of the dual specificity protein phosphatase, DsPTP1, through interactions with calmodulin. J. Biol. Chem. **279:** 848–858.

Zhang, D., and Yuan, Z. (2014). Molecular control of grass inflorescence development. Annu. Rev. Plant Biol. **65:** 553–578.

Zuo, J., and Li, J. (2014). Molecular genetic dissection of quantitative trait loci regulating rice grain size. Annu. Rev. Genet. **48:** 99–118.